1.1µm Backside Imager vs. Frontside Imager: an optics-dedicated FDTD approach

Flavien Hirigoyen[(a)], Jérôme Vaillant, Emilie Huss, Frederic Barbier, Jens Prima, François Roy, Didier Hérault
STMicroelectronics, 850 rue Jean Monnet, 38920 Crolles, France
[(a)] E-mail : flavien.hirigoyen@st.com
Tel. : (33) 4 7692 5464
Fax: (33) 4 7692 5331

***Abstract*—In 2009 the race to miniaturization and high performance of CMOS image sensors lead companies to propose 1.4µm pixels and to develop 1.1µm pixels with high signal to noise ratio even at low light level. At this scale diffraction effects of metallic interconnections of Frontside (FSI) technology become preponderant and can limit the quantum efficiency while degrading crosstalk. A promising technology to overcome these effects is the Backside (BSI) technology: the light passes through the back thinned side of the sensor and is not disturbed by the metallic windows. In this paper we propose to evaluate the optical performances of a 1.1µm BSI pixel compared to a 1.1µm FSI pixel using a Finite Difference Time Domain simulation we previously developed at STMicroelectronics. After a calibration of the BSI modeling on a realized and measured 1.4µm pixel, we will compare the spots sizes, the transmitted energies at silicon interface and the energy distribution inside the silicon of the BSI and FSI 1.1µm pixels.**

***Index Terms*—Backside imager, Frontside imager, Finite Difference Time Domain, Image Sensors, Optical Simulations**

I. Introduction

The Image Sensors market has experienced considerable growth over last decade due to the increasing demands of digital still and video cameras, security cameras, webcams, automotive, and mainly mobile cameras. These image sensors must follow an aggressive miniaturization trend to be easily embedded into smaller and smaller packages, at lower cost while keeping high levels of performances particularly at low light illumination. Among several performances criterions, photo-electron collection must be maximized without degrading the crosstalk, thus diffraction effects occurring at small pixel size must be rigorously evaluated.

In 2009 CIS companies must develop high performance 1.1µm pixels and at this scale the metallic apertures of the pixels of Frontside imagers induce diffraction effects which can lower the quantum efficiency and degrade the crosstalk. A promising alternative to overcome these effects is the Backside technology: the sensor is illuminated directly from the backside of the silicon substrate, and the waves can travel until the photodiode without being disturbed by metal lines. We have previously developed and calibrated at STMicroelectronics a 3D-modeling methodology based on Finite Difference Time Domain (FDTD) to simulate these diffraction effects for future small pixels [1]. We propose in this paper to compare with this FDTD-tool the optical performances of a 1.1µm Backside pixel vs. a 1.1µm Frontside pixel with aggressive design rule and process.

In the second part of this article we describe the FDTD methodology, the material modeling, the approximation of the diffuse-like source by plane waves, and the final signal calculation. Then in a third part we simulate the Quantum Efficiency of a 1.4µm Backside pixel developed and measured, in order to validate the model in a BSI technology.

Finally in a fourth part we simulate the optical performances of 2 advanced 1.1µm pixels: a first one designed in Frontside technology, and a second one designed in Backside technology. We will compare the spots shapes and the transmitted energies at silicon interface.

.

II. Methodology

Historically we started at STMicroelectronics the optical simulations modeling with a ray tracing based optical tool [2]. It was fast, easy to use and the Descartes laws were adapted to the description of the optical performances of pixels from 6µm down to 3µm. But below this scale the diffraction limit is reached and it becomes mandatory to take into account these effects. Thus we chose to adopt a more fundamental description based on Maxwell-Boltzmann modeling, and to compute it using FDTD-based software [3]. This modeling consists in importing the exact layout of the pixel into a realistic process. Each layer is constituted of a material which properties are described by a dispersive model. The structure is meshed in 2 interlaced grids made up of Yee cells and the plane waves propagations are computed by solving Maxwell-Boltzmann equations at each node until a steady state is reached [4][5][6]. A specific study has been done to approximate a diffuse-like source by weighted plane waves in order to get a realistic response of the sensor to a product-like illumination [7]. The intensity distribution of the light is obtained from the Poynting vector ($W.m^{-2}.Hz^{-2}$) which is the vector product of E-field ($V.m^{-1}.Hz^{-1}$) and H-field ($A.m^{-1}.Hz^{-1}$):

$$\vec{P}(f) = \frac{1}{2}.\mathrm{Re}\left[\vec{E}(f) \times \vec{H}(f)\right] \quad (1)$$

The final signal is obtained by calculating the 2D transmitted energy anywhere inside the structure on one hand, and the 3D absorbed energy in the silicon on the other hand.

$$T(f) = \frac{\iint P_z(f).dx.dy}{\iint S_z(f).dx.dy} \quad (2)$$

with T transmission, P_z z-component of Poynting and S_z power of source in z-direction, f frequency.

The 3D absorbed energy is calculated from the divergence of the Poynting vector:

$$A(f) = \frac{\iiint -real(\nabla\vec{P}(f)).dx.dy.dz}{\iint S_z(f).dx.dy} \quad (3)$$

This latter quantity will be the Optical Quantum Efficiency (OQE) since it corresponds to the absorbed photons in a defined volume. In order to suppress the oscillations due to the interferences inside the pixel optical stack, the Poyntings are averaged along +/-20nm in wavelength.

III. Calibration on a 1.4µm BSI pixel

This FDTD methodology has yet been calibrated on several FSI pixels and processes, but before making any comparison between advanced 1.1µm FSI and 1.1µm BSI pixels we must calibrate the simulator to a realized and measured 1.4µm BSI pixel [8]. Indeed we simulate the Optical Quantum Efficiency in diffuse-like illumination condition of a Backside structure (see Figure 1) at 450nm +/-20nm, 532nm +/-20nm and 633nm+/-20nm (see Figure 2). This structure is composed of a full Bayer pattern (GR, R, B and GB pixels), thus we can calculate the Optical Quantum Efficiency by summing the absorbed energy as in equation (3) pixel by pixel in volumes defined by doping implant zones. It is afterward possible to compare the complete Bayer pattern ∑OQE summation (see equation (4)) to the measured ∑QE (see equation (5)) and to have interpretations on diffusion/recombination of charges.

$$\sum OQE = A(GR) + A(R) + A(B) + A(GB) \quad (4)$$

$$\sum QE = QE(GR) + QE(R) + QE(B) + QE(GB) \quad (5)$$

This is illustrated in Figure 3 where simulated OQE and measured QE are compared, showing a good correlation of the total ∑OQE with ∑QE at the three wavelengths. We can see that the simulated OQE of the pixels corresponding to the peak response of the filters (B pixel at 450nm, GB and GR pixels at 532nm and R pixel at 633nm) are greater than the measured QE, while the OQE of the other pixels are smaller than the measured QE. This permits to quantify the amount of photo-generated carriers that diffuse to the adjacent pixels, and to locate the region in silicon where this phenomenon are suspected to occur, helping further analysis and improvement of process and technology at both back-end and front-end levels. It is too possible to couple these photonic distributions inside silicon into a TCAD electrical modeling tool for more advanced diffusion carriers analysis [9].

IV. 1.1µm FSI vs. 1.1µm BSI pixel

The FDTD simulator being calibrated on both FSI and BSI technologies we can use it in order to compare the potential optical performances of two 1.1µm pixels designed in FSI and BSI technologies.

The FSI pixel is designed with current most aggressive FSI design rules so that metal windows let light pass through the back-end, and the MOS transistors are situated to enable a competitive photodiode fill factor of about 40%.

The BSI pixel has similar design rules but the stack below the microlenses is adapted with realistic anti-reflective layers to maximize its transmission over the whole visible spectrum. The BSI stack height from microlenses bottom until silicon surface is reduced by approximately 30% regarding FSI stack height and both structures have an average refractive index of 1.6 at 550nm (see Figure 4). The simulated microlenses of the two structures are optimized to focus at silicon interface.

The simulation consists in comparing the transmission performances at silicon interface of the 2 pixels at 450nm +/-20nm, 532nm +/-20nm and 633nm +/-20nm, at F#=2.8. The spots at silicon interface and transverse propagations are on Figure 5, Figure 6 and Figure 7. FSI spots clearly seem to be disturbed at the three wavelengths rather than BSI spots are still circular. If we look to the silicon interface transmissions, the BSI structure shows significant optical gains at pixel maximum transmission (i.e. B pixel at 450nm, GR and GB pixels at 532nm and R pixels at 633nm), and optical crosstalk is improved (see Table 1): transmission is improved from 53% in blue to 32% in green and 33% in red, while color ratios are also substantially improved without modifying filters thicknesses (i.e. R/G(BSI) is 0.44xR/G(FSI) at 532nm).

V. Conclusion

In this paper we have presented an FDTD-based approach to describe optical performances of Backside technology over Frontside technology to anticipate future small 1.1µm pixels development. Since this tool has yet been calibrated on several precedent FSI pixels and technologies, we have demonstrated the validity of the methodology to a realized 1.4µm BSI pixel. Then we have used this model to rigorously describe the propagation of the light in product-use illumination conditions of 2 advanced 1.1µm pixels designed in FSI technology and BSI technology. This study has shown promising results of BSI technology from optics point of view: pixel peak responses are improved from 53% to 33% at the three wavelengths while optical crosstalk is substantially enhanced. These latter performances criterions are vital indicators to improve the signal-to-noise ratios of future small pixels at low light illumination conditions.

ACKNOWLEDGMENT

The author gratefully acknowledges Dr. James Pond and his team at Lumerical for their constant support in the optimization of the simulation tool.

REFERENCES

[1] F. Hirigoyen, A. Crocherie, J. Vaillant, and Y. Cazaux, "FDTD-based optical simulations methodology for CMOS image sensor pixels architecture and process optimization", Proc. of SPIE-IS&T Electronic Imaging, vol. 6816, 2008.

[2] J. Vaillant, F. Hirigoyen, "Optical simulation for CMOS imager microlens optimization", Proc. of the SPIE, Volume 5459, pp. 200-210, September 2004.

[3] Lumerical Solutions, Inc. Available: http://www.lumerical.com

[4] A. Taflove and S. C. Hagness, "Computational Electrodynamics: the finite-difference time-domain method, 2nd Edition", H. E. Schrank, Series Editor (Artech House, Boston, Ma, 2000).

[5] K. S. Yee, "Numerical solution of initial boundary value problems involving Maxwell's equations in isotropic media", IEEE Transactions on Antennas and Propagation, Vol. AP-14, number 3, pp. 302-307, 1966.

[6] A. Taflove and M. E. Brodwin (1975). "Numerical solution of steady-state electromagnetic scattering problems using the time-dependent Maxwell's equations". Microwave Theory and Technique,, IEEE Transactions on 23: 623–630

[7] J. Vaillant, A. Crocherie, F. Hirigoyen, A. Cadien, J. Pond, "Uniform Illumination and rigorous electromagnetic simulations applied to CMOS Image Sensors", Optics Express, Vol. 15, Issue 9, pp. 5494-5503, April 2007

[8] J. Prima, F. Roy, "Improved color separation for a backside illuminated image sensor with 1.4 µm pixel pitch", 2009 International Image Sensor Workshop (IISW), 25-29th June 2009

[9] A. Crocherie, P. Boulenc, F. Hirigoyen, J. Vaillant, C. Tavernier, "From photons to electrons: a complete 3D simulation flow for CMOS image sensor", ", 2009 International Image Sensor Workshop (IISW), 25-29th June 2009

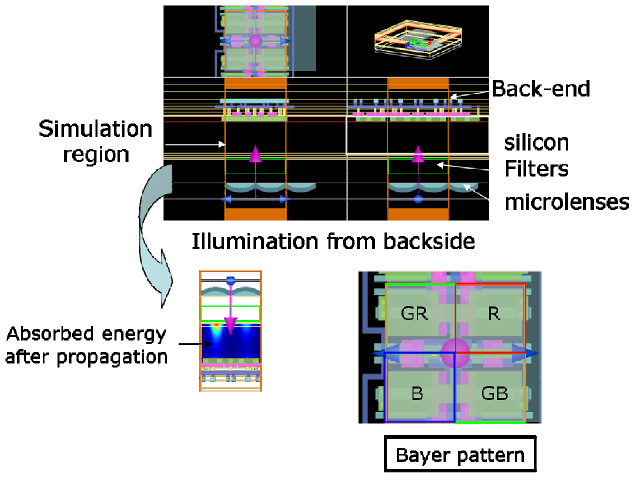

Figure 1: 3D simulated structure of 1.4µm BSI pixel and absorbed energy in silicon

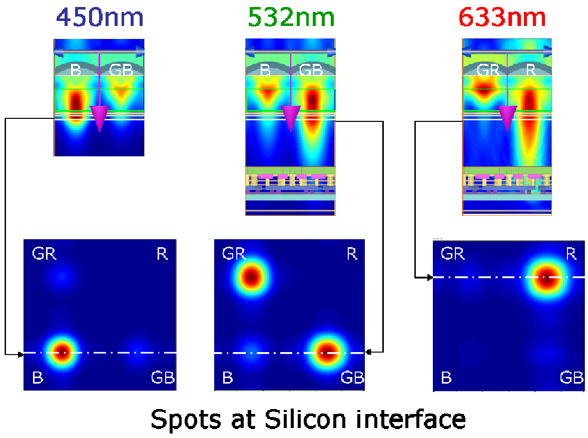

Figure 2: Poyntings vertical cuts and spots at silicon interface at 450nm, 532nm and 633nm of a 1.4µm BSI pixel

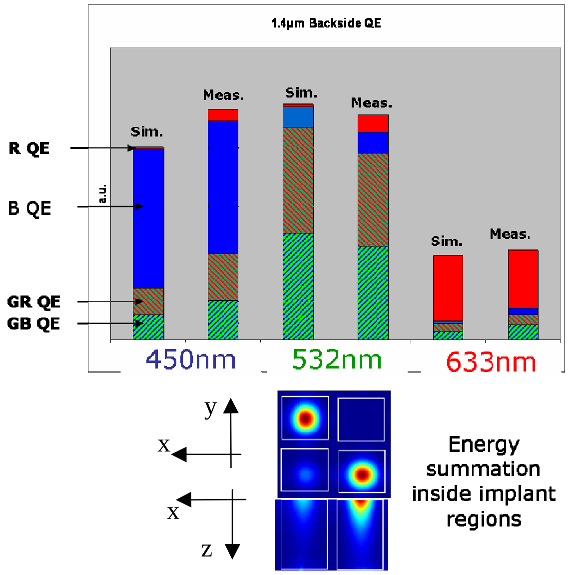

Figure 3: Comparison of simulated optical QE to measured QE of a 1.4µm BSI pixel at 450nm, 532nm, 633nm

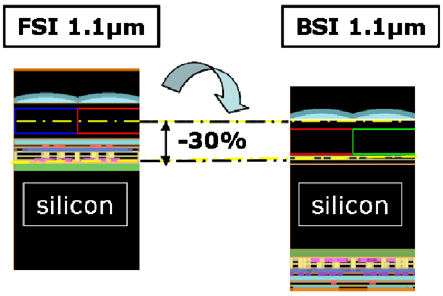

Figure 4: 1.1µm FSI process vs. 1.1µm BSI process

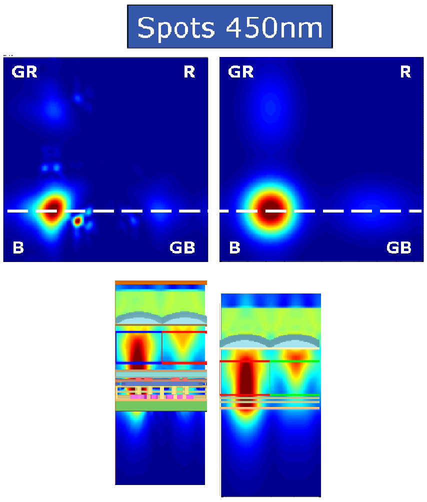

Figure 5: FSI vs. BSI: 1.1µm spots sizes at 450nm

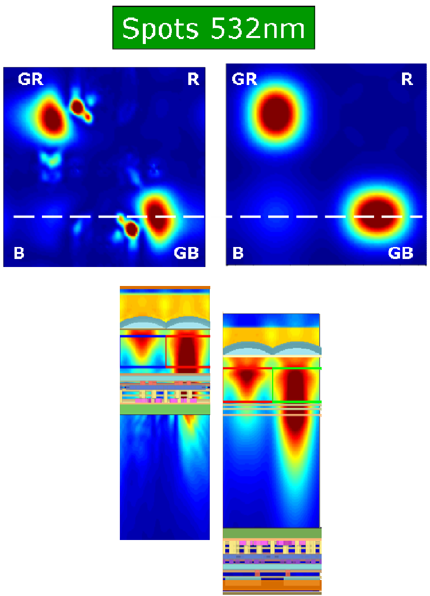

Figure 6: FSI vs. BSI: 1.1µm spots sizes at 532nm

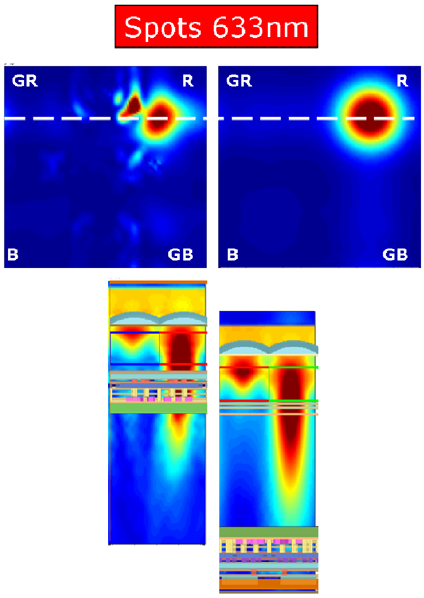

Figure 7 FSI vs. BSI: 1.1µm spots sizes at 633nm

Gains BSI vs. FSI	Color ratios		Pixel peak
450nm	G/B	R/B	B
	0.87	0.87	1.53
532nm	B/G	R/G	G
	1.00	0.44	1.32
633nm	B/R	G/R	R
	0.70	0.85	1.33

Table 1: Optical gain of 1.1µm BSI structure vs. FSI structure